Detergent-resistant membranes in HeLa cells. A comparative study with an electrochemical and lipidomic perspective

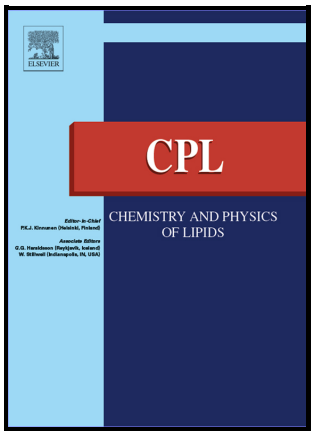

Anastasie Mateckaja, Martina Zatloukalová, Gabriel Gonzalez, Richard Masař, Lukáš Najdekr, Zdeněk Dostál, Vlastimil Dorčák, Jan Vacek

PII: S0009-3084(25)00045-3

DOI: https://doi.org/10.1016/j.chemphyslip.2025.105509

Reference: CPL105509

To appear in: *Chemistry and Physics of Lipids*

Received date: 7 October 2024
Revised date: 27 May 2025
Accepted date: 29 May 2025

Please cite this article as: Anastasie Mateckaja, Martina Zatloukalová, Gabriel Gonzalez, Richard Masař, Lukáš Najdekr, Zdeněk Dostál, Vlastimil Dorčák and Jan Vacek, Detergent-resistant membranes in HeLa cells. A comparative study with an electrochemical and lipidomic perspective, *Chemistry and Physics of Lipids,* (2025) doi:https://doi.org/10.1016/j.chemphyslip.2025.105509

Detergent-resistant membranes in HeLa cells. A comparative study with an electrochemical and lipidomic perspective

Anastasie Mateckaja[a], Martina Zatloukalová[a], Gabriel Gonzalez[b,c], Richard Masař[d], Lukáš Najdekr[d], Zdeněk Dostál[a], Vlastimil Dorčák[a], Jan Vacek[a,*]

[a] *Department of Medical Chemistry and Biochemistry, Faculty of Medicine and Dentistry, Palacky University, Hnevotinska 3, 775 15 Olomouc, Czech Republic*

[b] *Department of Neurology, Faculty of Medicine and Dentistry, Palacky University and University Hospital Olomouc, I. P. Pavlova 6, 779 00 Olomouc, Czech Republic*

[c] *Department of Experimental Biology, Palacky University Olomouc, Faculty of Science, Slechtitelu 27, 78371 Olomouc, Czech Republic*

[d] *Institute of Molecular and Translational Medicine, Palacky University Olomouc, Hnevotinska 5, 779 00 Olomouc, Czech Republic*

*) Corresponding author: J. Vacek (jan.vacek@upol.cz)

Abstract

Two procedures are compared for the isolation of detergent-resistant membranes (DRMs) from the HeLa model cell line. The isolation was based on application of Triton X-100 followed by 4 or 18 h ultracentrifugation in sucrose (5–42.5, % *w*) or Optiprep™ (10–25, % *w*) gradients. In the fractions obtained, the total amount of protein, cholesterol, and free thiols was evaluated using spectrophotometry. Increased protein as well as free thiol contents were demonstrated in higher density fractions. In contrast, the highest cholesterol levels were observed in light or medium heavy fractions with a low proportion of sucrose or Optiprep, especially after 18 h of centrifugation. For the sucrose gradient, we used voltammetric determination of the catalytic hydrogen evolution reaction at the Hg-electrode for individual fractions. The catalytic response, expressed as the height of the presodium wave, increased from light to heavy fractions corresponding to the protein content and/or other catalytically active species. The size of the DRMs or their associates ranged from 20 to 1000 nm, independently of the isolation protocol used. Proteins typically associated with DRMs such as caveolin and flotillin and characteristic for light and medium heavy gradient fractions, were determined using immunochemistry. We studied the subcellular localization of caveolin, flotillin, raftlin and transferrin, a control protein found intracellularly in the cytoplasm. Using confocal fluorescence microscopy, we confirmed the presence of caveolin and flotillin in the cytoplasmic membrane of HeLa cells. Raftlin was identified in both the membrane, and as part of the cell nucleus. We also performed untargeted

lipidomic LC-MS analysis of the individual fractions of sucrose ultracentrifugation gradient obtained after 18 h. The predominant lipid classes were phosphocholines and diacylglycerols. Apart from cholesterol and its ester, the rest of identified lipid classes was similar to that found in full HeLa cell lysates. The presented findings could be important for interpreting interlaboratory results and may be used as a guide for further studies on DRMs.

Keywords:

detergent-resistant membranes, cholesterol, Ellman's assay, ultracentrifugation, voltammetry, raftlin, lipidomics

1. Introduction

Membrane domains enriched with sphingolipids and cholesterol resist the action of non-ionic detergents (*e.g.* Triton X-100, Brij, or zwitterionic CHAPS) at low temperatures (London and Brown, 2000). Detergents increase the solubility of membranes and this occurs in three steps (Helenius and Simons, 1975): detergent incorporation, lamellar-micellar phase transition (formation of mixed micelles), and final solubilization (separation of proteins and lipid mixed micelles) (Lingwood and Simons, 2007). The undissolved membrane components contain cholesterol, sphingolipids and some proteins, mostly glycosylphosphatidylinositol (GPI)-anchored proteins (Brown and Rose, 1992). We refer to these domains as detergent-resistant membranes (DRMs) (Brown and London, 1997). They are characterized by low density and can be separated from the rest of the dissolved components using density gradient ultracentrifugation (Brown and Rose, 1992). Fragments of the plasma membrane isolated in this way represent the liquid-ordered (L_o) lipid phase (Ahmed et al., 1997; Brown and London, 1998b). In particular, the high concentration of sphingolipids and cholesterol in DRMs suggests that detergent-insoluble rafts in an L_o-like state, may coexist with the detergent-soluble Lα state domains in cell membranes (London and Brown, 2000).

The term lipid rafts (LRs) was established and reported in ref. (Simons and Ikonen, 1997). LRs are structural domains found in living cells whose components can be isolated as DRMs (Brown and London, 1998a). However, DRMs do not reflect the native membrane organization and cannot be strictly considered *in situ* LRs found in living cells and which may arise from lipid-lipid or lipid-protein interactions or the involvement of these domains in the cell membranes (Pike, 2009). DRMs domains contain specifically associated proteins (Brown and Rose, 1992): Src family protein tyrosine kinases (Arreaza et al., 1994; Dráberová and Dráber, 1993), GPI-linked proteins (Sargiacomo, 1993) and others. LRs in living cells have the ability to concentrate proteins and signalling molecules, their main function and, in this way their mutual interactions are supported (Pike, 2006). They serve as dynamic platforms for

receptor signalling, transport (Staubach and Hanisch, 2011a), immune response, pathogen recognition, and cytokine regulation (Barnett and Kagan, 2019; Varshney et al., 2016). These domains are also associated with some neurodegenerative (Sonnino et al., 2014) and cardiovascular (atherosclerosis development) (Rios et al., 2013) diseases, viral infections (Bukrinsky et al., 2020), and insulin resistance (Vainio et al., 2005).

This study compared two procedures for isolating DRMs from the HeLa model cell line. Isolation was based on the application of Triton X-100 detergent followed by ultracentrifugation in sucrose or Optiprep™ gradients. These media are among the most commonly used for DRMs isolation (Macdonald and Pike, 2005; Persaud-Sawin et al., 2009); for more details on the isolation aspects see refs (Brown, 2006; Lingwood and Simons, 2007; Schuck et al., 2006). In the DRM fractions isolated, the amount of total protein, cholesterol, and free thiol contents were evaluated using spectrophotometry. The particle distribution in individual fractions has been described by the dynamic light scattering (DLS). Proteins typically associated with DRMs were determined using immunochemistry followed by their subcellular localization in HeLa cells. The application of voltammetric and untargeted lipidomic LC-MS analysis for DRMs characterisation is discussed here for the first time.

2. Materials and Methods

2.1. Chemicals

Optiprep™ was obtained from Sigma Aldrich. The Total Cholesterol Assay Kit was purchased from Erba Lachema (cat# BLT00034). The chemiluminescence reagents and monoclonal antibody against flotillin-1 were from Santa Cruz Biotechnology (cat# sc-74566), polyclonal antibody against caveolin-1 was purchased from Cell Signaling Technology (cat# 3238), polyclonal antibody against raftlin was from Abcam (cat# ab233438) and monoclonal antibody against transferrin receptor was from Invitrogen (cat# 13-6800). Horseradish peroxidase-conjugated anti-rabbit IgG (cat# 7074S) and anti-mouse IgG (cat# 7076S) were obtained from Cell Signaling Technology. The total protein in each fraction was determined using a Pierce BCA Protein Assay Kit (Thermo Scientific, Rockford, IL, USA).

2.2. HeLa cells

HeLa cells were obtained from ECACC (No. 93021013 Human Negroid cervix epitheloid carcinoma cell line) *via* Sigma-Aldrich as the provider. Cells were cultivated in Minimum Essential Medium Eagle (Sigma Aldrich) supplemented with 10% foetal bovine serum (Serana), 100 units/ml of penicillin/0.1 mg/ml of streptomycin (Sigma Aldrich) and 1% non-

essential amino acids (Sigma Aldrich). The cells were incubated in a humidified incubator with a 5% CO_2 atmosphere at 37 °C, and passaged every 2 to 4 days. Approx. 150×10^6 cells were collected for each isolation of DRMs, except for samples for untargeted LC-MS lipidomic analysis where approx. 300×10^6 cells were used.

2.3. Method for the preparation of DRMs

The procedures were carried out on ice, and all reagents and tools were precooled to ≤ 4 °C. The cells were washed and scraped into PBS. They were pelleted by centrifugation for 2 min at 500 × *g*, and resuspended in 500 µL of lysis buffer with detergent (1 × TBS of pH 8, 1% Triton X-100) and incubated on ice for 30 min. The homogenate was centrifuged at 1000 × *g* for 10 min at 4 °C, and postnuclear supernatant (PNS) was removed and maintained on ice. The pellet was then once more resuspended in 500 µL of the lysis buffer with detergent and incubated on ice for 30 min. The homogenate was centrifuged at 1000 × *g* for 10 min at 4 °C, and PNS was removed and pooled with the first PNS. The final pellet was discarded. The supernatant was subjected to density gradient centrifugation with sucrose (details in Sec. 2.3.1.) or Optiprep (Sec. 2.3.2.). Blank tubes were prepared with 1 mL of the lysis buffer with detergent instead of PNS. Gradients were fractionated into 300 µL fractions.

2.3.1. Sucrose step density gradient

An equal volume (1 mL) of gradient buffer (1 × TBS, pH 8) containing 85 % sucrose and PNS were placed in the bottom of a 4 ml centrifuge tube. 1 mL of 35% sucrose in TBS was then overlaid, followed by 1 mL of 5% sucrose in TBS. The tube was centrifuged for 4 or 18 hours at 200 000 × *g* (4 °C) using a 50.4 Ti rotor in a Beckman ultracentrifuge.

2.3.2. Optiprep step density gradient

The Optiprep™ density gradient was prepared in the same manner as the sucrose density gradient. An equal volume (1 mL) of gradient buffer (1 × TBS, pH 8) containing 50 % Optiprep and PNS were placed in the bottom of a 4 mL centrifuge tube. 1 mL of 20% Optiprep in TBS was then overlaid, followed by 1 mL of 10% Optiprep in TBS. The tube was centrifuged for 4 or 18 hours at 200 000 × *g* (4 °C) using a 50.4 Ti rotor in a Beckman ultracentrifuge.

2.4. Characterization of isolated detergent-resistant lipid membranes

2.4.1. SDS-PAGE and Western blot analysis

As protein concentration does not provide an accurate baseline parameter for comparison across fractions, an equal sample volume loading was used for the western blot. This accounts for the differential separation of proteins into specific fractions after density ultracentrifugation.

Samples of DRMs were subjected to electrophoresis through 10% SDS-polyacrylamide gel. Proteins were transferred to a polyvinylidene difluoride membrane by electroblotting, and the membranes were probed with primary antibodies, including mouse monoclonal flotillin-1 antibody, rabbit polyclonal caveolin-1 antibody, rabbit polyclonal raftlin antibody, and mouse monoclonal transferrin receptor antibody. Primary antibodies were visualized with anti-rabbit or anti-mouse IgG-HRP secondary antibodies (# 7074S; #7076S; Cell Signaling Technology) using a chemiluminescent reaction, and the blots were imaged using a G:Box Chemi-XX6 gel doc system (Syngene, Cambridge, UK). The relative band intensities were evaluated by densitometric analysis using the software ImageJ (National Institutes of Health, Bethesda, MD, USA).

2.4.2. Dynamic light scattering

The samples were prepared as described above. DLS measurements were performed using a Zetasizer Nano ZSP (Malvern Panalytical, Malvern, UK) at 20 °C.

2.4.3. Ellman's assay

Determination of thiol compounds by Ellman's assay is based on the reaction with 5-5′-dithio-bis-(2-nitrobenzoic acid), DTNB (Dietz and Rubinstein, 1972). DTNB forms 5-thionitrobenzoic acid (TNB) and a mixed disulphide. A stock solution of Ellman's reagent was prepared with a final concentration of 50 mM sodium acetate and 2 mM DTNB in molecular biology grade water. Samples containing isolated DRMs were mixed with Ellman's reagent in the presence of 1 M Tris buffer (pH 8) at room temperature in a ratio 1:1:2 (*v*), respectively. Absorption at 412 nm was read against blank fractions and DTNB reagent.

2.4.4. Electrochemical analysis

Electrochemical measurements were carried out at laboratory temperature with a μAutolab III analyzer (EcoChemie) in a three-electrode setup with a hanging mercury drop electrode (HMDE, area 0.4 mm^2) as the working electrode, an Ag|AgCl|3 M KCl electrode as the reference, and a glassy carbon rod as the auxiliary electrode. The pH measurements were carried out with an HI 2211 pH/ORP Meter (Hanna Instruments).

2.4.5. Immunofluorescence staining with confocal microscopy

Hela cells were seeded in a density of 13000 cells/300 µL well in µ-Slide 8 (IBIDI) slides. After 24 hours, cells were fixed and stained with an antibody (Steigerova et al., 2010). Medium from cells was briefly aspirated, and ice-cold acetone: ethanol 1:1 was added for 10 min. After 10 min, fixed cells were dried out. Subsequently, dried cells were hydrated with PBS-T solution for 3 minutes followed by blocking in 1% BSA in PBS-T for 30 min. After washing with PBS-T, the primary antibodies were applied and kept at 4 °C overnight. The next day, slides were washed 5 times and anti-mouse IgG conjugated with Alexa Fluor 488 or anti-rabbit IgG conjugated with Alexa Fluor 488 (diluted 1:1000; Invitrogen) were used for 30 min at room temperature, and 60 min at 4 °C. After the incubation, cells were washed with PBS-T, then PBS followed by staining of cell nuclei with propidium iodide (1 µg/ml) for 15 min at r.t. Subsequently, cells were then washed with deionized distilled water, and Fluor safe media was added. Immunostained cells were observed by laser-scanning confocal microscopy with a Leica TCS SP2 (Leica Microsystems, Wetzlar, Germany) equipped with Argon-Krypton 476-514 nm, Helium-Neon 543 and Neon 633 nm lasers. Images were acquired using an HCX PL APO CS 63.0x1.40 OIL immersion objective. The resulting images were processed in the software ImageJ (Fiji).

2.4.6. LC-MS untargeted lipidomic analysis

2.4.6.1. Internal standards and their preparation

The internal standards were prepared by mixing 28.5 mL of isopropanol with 1.5 mL of SPLASH™ LIPIDOMIX™ Mass Spec Standard (330707, Avanti Polar Lipids, Alabaster, AL, USA). Subsequently, 15.8 µL of deuterated Cer(d18:1-d7/15:0), internal standard from Avanti Polar Lipids, was added to the prepared isopropanol mixture. The exact composition of final internal standard mixture was as follows: ChE 18:1-d7, 356.1 µg/mL; PC (15:0/18:1-d7), 160.7 µg/mL; Cholesterol-d7, 98.4 µg/mL; TG (15:0/18:1-d7/15:0), 57.3 µg/mL; SM (d18:1/18:1-d9), 30.9 µg/mL; LPC 18:1-d7, 25.5; DG (15:0/18:1-d7), 9.4 µg/mL; PI (15:0/18:1-d7), 9.1 µg/mL; PE (15:0/18:1-d7), 5.7 µg/mL; LPE 18:1-d7, 5.3 µg/mL; PS (15:0/18:1-d7) 4.2 µg/mL; PA (15:0/18:1-d7), 7.4 µg/mL; PG (15:0/18:1-d7), 29.1 µg/mL; Cer (d18:1-d7/15:0); 1 mg/mL.

2.4.6.2. Lipid raft extraction and LC-MS analysis

The samples of DRMs were processed by modified Bligh and Dyer extraction (Bligh and Dyer, 1959; Ulmer et al., 2018) as follows. To 300 µL of the gradient fraction was added 333 µL of MeOH (vortex for 10 s) and 333 µL of chloroform. The samples were placed in the shaker for

10 min, 1400 rpm, at room temperature. Afterwards, the samples were left on the ice for 10 min, followed by a round of shaking for 10 min, 1400 rpm at room temperature. Samples were centrifuged (22400 × *g*, 10 min at 4 °C), and 320 µL of the lower (organic) phase was transferred into the new tubes. To re-extract lipid fractions, 200 µL of water, 500 µL of MeOH and 500 µL of chloroform were used. Again, the samples were left on the ice for 10 min, followed by another round of shaking for 10 min, 1400 rpm at room temperature. After the shaking, the samples were centrifuged (22400 × *g*, 10 min at 4 °C). The chloroform layer was withdrawn (480 µL), added to the collected organic phase and dried in a vacuum concentrator. Finally, the dry pellet was resuspended in 100 µL of final internal standard mixture (see previous section), centrifuged (22400 × *g*, 10 min at 4 °C), and 90 µL of the samples were transferred to an HPLC vial. Blank samples were prepared using the same procedure instead of gradient fraction LCMS water was used.

The samples were analysed by ultrahigh-performance liquid chromatography coupled (Vanquish Horizon Separation UHPLC system, ThermoFisher Scientific, MA, USA) with mass spectrometry (Orbitrap Ascend, Thermo FisherScientific, MA, USA). The chromatographic separation was done on a reversed-phase column (Accucore C30 column, 150 mm × 2.1 mm, 2.6 µm; Thermo Fisher Scientific, MA, USA). The constitution of mobile phase A was 20 mM ammonium formate in 60:40 acetonitrile:water, and mobile phase B consisted of 20 mM ammonium formate in 85.5:9.5:5 isopropanol: acetonitrile:water. Gradient: t= 0.0, 20% B; t= 2.5, 20% B, t= 2.6, 55% B; t= 12, 60% B; t= 12.1, 80% B; t= 19.0, 90% B; t= 21.0, 100% B; t= 23.0, 100% B; t= 23.1, 20% B; t= 30.0, 20% B. All changes were linear (curve = 5), and the flow rate was 0.400 $mL.min^{-1}$. The column temperature was 55 °C, and the injection volume was 2 µL. Data were acquired simultaneously in positive and negative ionisation modes (150–2000 *m*/*z*) with a resolution of 120,000 (FWHM at *m*/*z* 200). Ion source parameters: sheath gas = 50 arbitrary units, auxiliary gas = 10 arbitrary units, sweep gas = 0 arbitrary units, spray voltage = 3.5 kV (positive ion)/2.5 kV (negative ion), capillary temp. = 325 °C, aux. gas heater temp. = 350 °C. The data were acquired cycle of one MS1 full-scan followed by data dependent MS^2 scans (DDA-MS^2) with cycle length of 600 milliseconds. The detailed settings were as follows: mass resolution =22,500 (FWHM at *m*/*z* 200); isolation width = 1.6 *m*/*z*; stepped normalised collision energies (stepped NCE) = 15, 35, 70. Thermo Tune Plus (4.2.4310.9) software controlled the instrument. All data were acquired in profile mode (Jankevics et al., 2021). Data were processed and evaluated using Compound Discoverer 3.4 software (Thermo Fisher Scientific, MA, USA). For other details see Supplementary Information.

Structural elucidation, comparison of fragmentation spectra with databases and fragmentation prediction of annotated diacylglycerols were verified using Mass Frontier 8.1 software (Thermo Fisher Scientific, MA, USA).

3. Results

The isolation was based on the application of the Triton X-100 detergent, followed by 4 or 18 h ultracentrifugation in gradients of sucrose (5–42.5, % *w*) or Optiprep™ (10–25, % *w*) according to a described methodology (Macdonald and Pike, 2005; Persaud-Sawin et al., 2009). Two gradient systems were chosen in order to compare the interference limits for individual analytical end-points. Numbering and colour identification of the light (beige), medium heavy (light green), and heavy (dark green) fractions are shown in Figure 1A. For clarity, this identification system is used in all the presented graphics.

After ultracentrifugation, DRMs could be identified visually as white coloured semi-transparent rings or zones (Fig. 1A, highlighted in orange). This phenomenon was more noticeable for the sucrose fractions than for the Optiprep fractions, in which the particle distribution was visually confirmed throughout the gradient. The distribution of DRM particles for both selected gradients was studied using DLS. The size of DRMs or their associates was found to range between 20 and 1000 nm, independently of the isolation protocol used. DLS profiles are shown for selected fraction 4 in Figure 1B. In this fraction, which was rich in cholesterol (see below), particle sizes between 20 and 450 nm predominated.

Furthermore, we evaluated the amount of total protein, cholesterol and free thiols in the fractions using spectrophotometric methods (Fig. 2). In accordance with the original isolation protocols (Macdonald and Pike, 2005; Persaud-Sawin et al., 2009), an increased total protein content was demonstrated in the heavier, higher density fractions (Fig. 2A,B). In contrast, the highest cholesterol levels were observed in light or medium heavy fractions, with a low content of sucrose or Optiprep, especially after 18 h of centrifugation. The levels of free thiols were determined using the Ellman's reaction (Fig. 2C).

We also applied voltammetric determination of the catalytic hydrogen evolution reaction (CHER) at the Hg-electrode for individual fractions (Fig. 2D). The CHER voltammetric response, expressed as presodium wave height (Δi) (Dorčák et al., 2024; Mader et al., 2001), is shown in the inset of Figure 2D. The value of Δi increased from light to heavy fractions, which corresponds to an increasing protein content and/or thiols localized at the surface of DRMs (Fig. 2D). Unlike the methods for determining proteins, cholesterol, and thiols, the electrochemical approach can only be used for the sucrose gradient. Interferences

were observed for the Optiprep gradient (not shown). Optiprep is a non-ionic organoiodide compound, iodixamol (Ford et al., 1994).

In further experiments, we focused on identifying proteins that occur in cytoplasmic lipid nanodomains. Using immunochemical methods, we determined proteins typically associated with DRMs, such as caveolin (Anderson and Jacobson, 2002; Rothberg et al., 1992), flotillin (Bickel et al., 1997; Langhorst et al., 2005) and raftlin (Saeki et al., 2003; Staubach and Hanisch, 2011b). The occurrence of flotillin-1 marker was confirmed for light and medium heavy gradient fractions (Fig. 3). This is consistent with the increased content of cholesterol in these lipid raft fractions, see Figure 2A,B. For caveolin-1, a broader distribution among fractions was confirmed, mainly for fractions of the sucrose gradient (Fig. 3C).

In addition, we examined the subcellular localization of caveolin, flotillin, raftlin and also transferrin which served as a control protein localized intracellularly in the cytoplasm (MacGillivray et al., 1998), as shown in Figure 4. Using confocal fluorescence microscopy, the presence of caveolin and flotillin in the plasma membrane of HeLa cells was confirmed *in situ*. Raftlin was not only identified in the cytoplasmic membrane, but also in the structures of cell nuclei.

Finally, we performed untargeted lipidomic LC-MS analysis in individual fractions after 18 h ultracentrifugation with sucrose gradient, which was compared with the lipidomic profile of whole HeLa cell lysate (Fig. 5). The Optiprep gradient was not investigated, because of its interference with LC-MS analysis not allowing high-quality quantification (data not shown). By utilising high-resolution MS and the MS^2 data-dependent acquisition mode, we putatively annotated 822 lipids in both positive and negative ESI modes. The annotation was based on spectral matching with the LipidSearch spectral library (Thermo Fisher Scientific, MA, USA). Phosphocholines (PC) were the most diverse and the second most abundant lipid class through the fractions based on peak areas and the number of annotations (n=432). After normalisation with internal standards, diacylglycerols (DG) emerged as the predominant class in terms of estimated molar concentrations. Cholesterol (Chol), lysophosphocholines (LPC), phosphoethanolamines (PE), sphingomyelins (SM), ceramides (Cer), and phosphatidic acids (PA) were quantified at concentrations approximately one order of magnitude lower than those of DG and PC. Trace amounts of hexosyl-ceramides (HexCer), lysophosphatidylethanolamines (LPE), phosphatidylglycerols (PG), phosphatidylinositols (PI) and cholesterol ester (ChE) were also detected; ChE was restricted to the lightest fractions.

4. Discussion

In this study, the model and well-established HeLa cell line (Gillet et al., 2013) was used for DRM isolation. The obtained DLS data (Fig. 1B) are consistent with a study on the isolation of DRMs from rat neuronal membranes using Triton X-100/Brij 96 detergents (Chen et al., 2009). The size profile of isolated DRMs does not directly correspond to the size of specific and functional lipidoprotein nanodomains, lipid rafts, which are found *in situ* in the plasma membrane of the cell. They are usually below 100 nm in size (De Wit et al., 2015).

The distribution of total protein and cholesterol in the fractions is consistent with original observations (Macdonald and Pike, 2005; Persaud-Sawin et al., 2009). Free thiol levels were determined using Ellman's reaction (Dietz and Rubinstein, 1972), and correspond to the total protein content (Figs 2A-C). This indicates that these are most likely cysteinyl residues of proteins or peptides, because free thiol low-molecular-weight (LMW) compounds have not been identified in lipid cell membranes. Ellman's reaction is selective for sulfhydryl groups, which are uncommon in mammalian lipids (Harwood and Nicholls, 1979). The increased SH group contents in the heavier fractions should be considered for manipulation with such DRM samples, as they may be subject to oxidation and may generally be more reactive towards electrophilic reagents (Vacek et al., 2022). With the development of proteomic methods that have been applied to the study of DRMs or LRs (Barrera and Robinson, 2011), it could be worthwhile in the future to compare the protein profiles of low- and high-density fractions.

Electrochemical analysis based on CHER was used for the first time for lipid membrane analysis (Fig. 2D). The voltammetric response Δi directly corresponded to the protein and thiol content. CHER is based on the catalytic contribution of chemical forms that contain functional groups with labile protons such as amino and/or thiol compounds. With peptides and proteins, Cys, His, Lys, and Arg residues were found catalytically active (Vacek et al., 2023). In addition to biopolymers such as including nucleic acids (Paleček and Bartošík, 2018), LMW-substances may also be involved in CHER, *e.g.* cysteamine (Dorčák et al., 2024; Novák et al., 2021). Simple lipid compounds and detergents do not usually contribute to CHER (Vacek et al., 2016). The results here also indicate the possibility of adsorption/immobilization of DRMs on electrode surfaces, in our case the hydrophobic Hg surface (Fig. 2D). This could be used for the development of new detection and manipulation platforms for DRMs analysis and study of multicomponent-lipid membrane interactions (Steinem and Janshoff, 2010).

We also used immunochemical methods to identify the proteins (caveolin, flotillin, and raftlin) that occur in cytoplasmic lipid nanodomains (Anderson and Jacobson, 2002; Bickel et al., 1997; Langhorst et al., 2005; Rothberg et al., 1992; Saeki et al., 2003; Staubach and Hanisch, 2011b). The occurrence of flotillin-1 was confirmed in light and medium heavy gradient

fractions and caveolin-1 was more broadly distributed among the fractions. This finding could indicate that flotillin-1 is more specific for identification of cholesterol-rich fractions of DRMs. Raftlin was identified in both the cytoplasmic membrane and cell nucleus (Fig. 4). This phenomenon which could be related to the subcellular translocation ability of raftlin (Watanabe et al., 2011) should be investigated in more depth in future studies using HeLa cells.

Each of the isolation procedures demonstrated here provides unique characteristics including local maxima (Fig. 2). The choice of density gradient will depend on its interference with the analytical method used. However, the highest cholesterol recovery was observed for both gradients in the case of 18 h-long ultracentrifugation where there was a proportional decrease in cholesterol content towards the heavier fractions. Based on these findings, use of the longer ultracentrifugation time is probably necessary for proper collection of cholesterol-rich microdomains. For a 4 h-long procedure, they are not sufficiently separated from other DRMs. We have limited knowledge about the protein (Barrera and Robinson, 2011) and lipid (Dawson, 2021; Harant et al., 2023; Kim et al., 2021; Ogiso et al., 2015; Pike et al., 2005; Qin et al., 2021; Simons and Gerl, 2010) composition of DRMs, caveolae or LRs.

We further performed LC-MS untargeted lipidomic analysis in the individual fractions of sucrose gradient and in the full HeLa cell lysate (Fig. 5). It was found that there is a proportional distribution among lipid classes, only for medium heavy fractions we found lipids in higher estimated concentration. The lipidic pattern of DRMs was similar to that found in the whole HeLa cell lysate, with respect to the dilution after ultracentrifugation. Cholesterol ester was identified exclusively in light (1-5) fractions, which agrees with distribution of the total cholesterol shown in Figure 2B. Based on the LC-MS analysis, the highest cholesterol content was observed for fraction 1 (125 ± 10 µM; estimated concentration), followed by stepwise decrease to heavier fractions (Fig. 5). Similarly, cholesterol followed by glycerophospholipids (*e.g.* PC, PI or PS) was earlier also identified as predominant lipids in pooled lipid fractions of HeLa cells (Harant et al., 2023). Regarding quantitative data, the estimated concentration of sphingomyelin in Triton X-100 rafts was the highest followed by PE and PC. The relative cholesterol concentration was ~47 % of the lipid composition compared to glycerophospholipids in the Triton X-100-resistant rafts (Pike et al., 2005). Cholesterol was also the most abundant class among lipids in the detergent-resistant fraction from the silica bead-coated membrane. Then, the second most abundant lipid subclasses were sphingomyelins and phosphatidylcholines. Lipidic profile in detergent resistant membranes was rich for cholesterol and quite similar as in whole cells (Ogiso et al., 2015), which agrees with our findings.

5. Conclusions

The results show that the distribution of DRMs and their properties are unique for each selected gradient ultracentrifugation profile. This is essential for interpreting interlaboratory results, and may be a guide for further studies on DRMs. In addition to comparative data based on two gradient procedures, application of CHER-based electrochemical approach is also described here. This proof-of-concept can be further expanded with respect to the analysis of proteins localized on DRM surfaces. Untargeted lipidomics data enhanced our knowledge about chemical composition of DRMs in the HeLa cell model.

Abbreviations

5-5′-dithio-bis-(2-nitrobenzoic acid) (DTNB)
5-thionitrobenzoic acid (TNB)
bovine serum albumin (BSA)
catalytic hydrogen evolution reaction (CHER)
ceramides (Cer)
cholesterol (Chol)
cholesterol ester (ChE)
detergent-resistant membrane (DRM)
diacylglycerols (DG)
dynamic light scattering (DLS)
data-dependent acquisition (DDA)
electrospray ionization (ESI)
free fatty acids (FA)
hexosyl ceramides (HexCer)
lipid raft (LR)
liquid chromatography-mass spectrometry (LC-MS)
low-molecular-weight (LMW)
lysophosphocholines (LPC)
lysophosphoethanolamines (LPE)
Metabolomics standards initiative (MSI)
phosphate-buffered saline (PBS) with Tween (PBS-T)
phosphatidylglycerol (PG)
phosphatidylinositol (PI)

phosphocholines (PC)
phosphoethanolamines (PE)
phosphatidic acid (PA)
postnuclear supernatant (PNS)
sphingomyelins (SM)
triacylglycerols (TG)
tris-buffered saline (TBS)

Acknowledgements

The authors gratefully acknowledge the financial support of Palacky University, Young Researcher Grants (UP JG_2023_006 and JG_2024_022) and internal grant (IGA_LF_2024_011). The authors are indebted to Ben Watson-Jones MEng and Alexander Oulton PhD for language correction.

Declaration of competing interests

The authors declare that they have no known competing financial interests or personal relationships that could have appeared to influence the work reported in this paper.

CRediT authorship contribution statement

Anastasie Mateckaja: Methodology – DRMs isolation and their detailed characterization. Martina Zatloukalova: Methodology – special focus on dynamic light scattering, Writing – review & editing, statistical data processing. Gabriel Gonzalez: Methodology – confocal fluorescence microscopy. Richard Masař: Methodology – lipidomic analysis and data processing, Writing – review & editing. Lukáš Najdekr: Methodology – lipidomic analysis and data processing, Writing – review & editing. Zdeněk Dostál: Methodology – HeLa cell line cultivation. Vlastimil Dorčák: Methodology – electrochemical analysis, Writing – review & editing. Jan Vacek: Conceptualization, Methodology – literature search, Writing – original draft, Writing – review & editing, Supervision, Project administration.

Authors contribution

A.M. and M.Z. performed experiments on the isolation of DRMs and the biochemical methodology, G.G. performed cell fluorescence imaging, L.N. performed sample characterization and data processing, Z.D. performed HeLa cell cultivation, V.D. performed electrochemical sensing, and J.V. designed the study and wrote the manuscript.

Supplementary Information Content:

Raw LC-MS lipidomic data and workflow settings, including estimated lipid concentrations.

References

Ahmed, S.N., Brown, D.A., London, E., 1997. On the Origin of Sphingolipid/Cholesterol-Rich Detergent-Insoluble Cell Membranes: Physiological Concentrations of Cholesterol and Sphingolipid Induce Formation of a Detergent-Insoluble, Liquid-Ordered Lipid Phase in Model Membranes. Biochemistry 36, 10944-10953.

Anderson, R.G.W., Jacobson, K., 2002. Cell biology: A role for lipid shells in targeting proteins to caveolae, rafts, and other lipid domains. Science 296, 1821-1825.

Arreaza, G., Melkonian, K.A., LaFevre-Bernt, M., Brown, D.A., 1994. Triton X-100-resistant membrane complexes from cultured kidney epithelial cells contain the Src family protein tyrosine kinase p62yes. J. Biol. Chem. 269, 19123-19127.

Barnett, K.C., Kagan, J.C., 2019. Lipids that directly regulate innate immune signal transduction. Innate Immun. 26, 4-14.

Barrera, N.P., Robinson, C.V., 2011. Advances in the Mass Spectrometry of Membrane Proteins: From Individual Proteins to Intact Complexes. Ann. Rev. Biochem. 80, 247-271.

Bickel, P.E., Scherer, P.E., Schnitzer, J.E., Oh, P., Lisanti, M.P., Lodish, H.F., 1997. Flotillin and epidermal surface antigen define a new family of caveolae- associated integral membrane proteins. J. Biol. Chem. 272, 13793-13802.

Bligh, E.G., Dyer, W.J., 1959. A rapid method of total lipid extraction and purification. Can. J. Biochem. Physiol. 37, 911-917.

Brown, D.A., 2006. Lipid rafts, detergent-resistant membranes, and raft targeting signals. Physiology (Bethesda) 21, 430-439.

Brown, D.A., London, E., 1997. Structure of Detergent-Resistant Membrane Domains: Does Phase Separation Occur in Biological Membranes? Biochemi. Biophys. Res. Commun. 240, 1-7.

Brown, D.A., London, E., 1998a. Functions of lipid rafts in biological membranes. Ann. Rev. Cell Develop. Biol. 14, 111-136.

Brown, D.A., London, E., 1998b. Structure and Origin of Ordered Lipid Domains in Biological Membranes. J. Membr. Biol. 164, 103-114.

Brown, D.A., Rose, J.K., 1992. Sorting of GPI-anchored proteins to glycolipid-enriched membrane subdomains during transport to the apical cell surface. Cell 68, 533-544.

Bukrinsky, M.I., Mukhamedova, N., Sviridov, D., 2020. Lipid rafts and pathogens: the art of deception and exploitation: Thematic Review Series: Biology of Lipid Rafts. J. Lipid Res. 61, 601-610.

Dawson, G., 2021. Isolation of lipid rafts (detergent-resistant microdomains) and comparison to extracellular vesicles (exosomes), Method. Mol. Biol., pp. 99-112.

De Wit, G., Danial, J.S.H., Kukura, P., Wallace, M.I., 2015. Dynamic label-free imaging of lipid nanodomains. Proc. Natl. Acad. Sci. U.S.S. 112, 12299-12303.

Dietz, A.A., Rubinstein, H.M., 1972. Standardization of the Ellman reaction. Clin. Biochem. 5, 136-138.

Dorčák, V., Kroutil, O., Kabeláč, M., Janata, J., Vacek, J., 2024. Cysteamine Chemisorption at Mercury-Solution Interfaces in the Context of Redox and Microdissociation Equilibria. Langmuir 40, 6253−6260.

Dráberová, L., Dráber, P., 1993. Thy-1 glycoprotein and src-like protein-tyrosine kinase p53/p56lyn are associated in large detergent-resistant complexes in rat basophilic leukemia cells. Proc. Natl. Acad. Sci. U.S.A. 90, 3611-3615.
Ford, T., Graham, J., Rickwood, D., 1994. Iodixanol: A Nonionic Iso-osmotic Centrifugation Medium for the Formation of Self-Generated Gradients. Anal. Biochem. 220, 360-366.
Gillet, J.P., Varma, S., Gottesman, M.M., 2013. The clinical relevance of cancer cell lines. J. Natl. Cancer Inst. 105, 452-458.
Harant, K., Čajka, T., Angelisová, P., Pokorná, J., Hořejší, V., 2023. Composition of raft-like cell membrane microdomains resistant to styrene-maleic acid copolymer (SMA) solubilization. Biophys. Chem. 296, 106989.
Harwood, J.L., Nicholls, R.G., 1979. The plant sulpholipid-- a major component of the sulphur cycle. Biochem Soc Trans 7, 440-447.
Helenius, A., Simons, K., 1975. Solubilization of membranes by detergents. Biochim. Biophys. Acta - Rev. Biomembr. 415, 29-79.
Chen, X., Jayne Lawrence, M., Barlow, D.J., Morris, R.J., Heenan, R.K., Quinn, P.J., 2009. The structure of detergent-resistant membrane vesicles from rat brain cells. Biochim. Biophys. Acta - Biomembr. 1788, 477-483.
Jankevics, A., Jenkins, A., Dunn, W.B., Najdekr, L., 2021. An improved strategy for analysis of lipid molecules utilising a reversed phase C30 UHPLC column and scheduled MS/MS acquisition. Talanta 229.
Kim, Y.C., Lee, J., Lee, D.W., Jeong, B.H., 2021. Large-scale lipidomic profiling identifies novel potential biomarkers for prion diseases and highlights lipid raft-related pathways. Veter. Res. 52, 105.
Langhorst, M.F., Reuter, A., Stuermer, C.A.O., 2005. Scaffolding microdomains and beyond: The function of reggie/flotillin proteins. Cell. Mol. Life Sci. 62, 2228-2240.
Lingwood, D., Simons, K., 2007. Detergent resistance as a tool in membrane research. Nat. Prot. 2, 2159-2165.
London, E., Brown, D.A., 2000. Insolubility of lipids in Triton X-100: physical origin and relationship to sphingolipid/cholesterol membrane domains (rafts). Biochim. Biophys. Acta - Biomembr. 1508, 182-195.
Macdonald, J.L., Pike, L.J., 2005. A simplified method for the preparation of detergent-free lipid rafts. J. Lipid Res. 46, 1061-1067.
MacGillivray, R.T.A., Moore, S.A., Chen, J., Anderson, B.F., Baker, H., Luo, Y., Bewley, M., Smith, C.A., Murphy, M.E.P., Wang, Y., Mason, A.B., Woodworth, R.C., Brayer, G.D., Baker, E.N., 1998. Two High-Resolution Crystal Structures of the Recombinant N-Lobe of Human Transferrin Reveal a Structural Change Implicated in Iron Release. Biochemistry 37, 7919-7928.
Mader, P., Veselá, V., Dorčák, V., Heyrovský, M., 2001. The "presodium" hydrogen evolution at the dropping mercury electrode catalysed by simple cysteine peptides. Collect. Czech. Chem. Commun. 66, 397-410.
Novák, D., Vrba, J., Zatloukalová, M., Roubalová, L., Stolarczyk, K., Dorčák, V., Vacek, J., 2021. Cysteamine assay for the evaluation of bioactive electrophiles. Free Radic. Biol. Med. 164, 381-389.
Ogiso, H., Taniguchi, M., Okazaki, T., 2015. Analysis of lipid-composition changes in plasma membrane microdomains. J. Lipid Res. 56, 1594-1605.
Paleček, E., Bartošík, M., 2018. Intrinsic Electrocatalysis in DNA. ChemElectroChem 5, 936-942.
Persaud-Sawin, D.-A., Lightcap, S., Harry, G.J., 2009. Isolation of rafts from mouse brain tissue by a detergent-free method. J. Lipid Res. 50, 759-767.

Pike, L.J., 2006. Rafts defined: a report on the Keystone symposium on lipid rafts and cell function. J. Lipid Res. 47, 1597-1598.
Pike, L.J., 2009. The challenge of lipid rafts. J. Lipid Res. 50, S323-S328.
Pike, L.J., Han, X., Gross, R.W., 2005. Epidermal growth factor receptors are localized to lipid rafts that contain a balance of inner and outer leaflet lipids: A shotgun lipidomics study. J. Biol. Chem. 280, 26796-26804.
Qin, C., Pan, M., Han, X., 2021. A detergent-free method for preparation of lipid rafts for the shotgun lipidomics study, Method. Mol. Biol., pp. 27-35.
Rios, F.J.O., Ferracini, M., Pecenin, M., Koga, M.M., Wang, Y., Ketelhuth, D.F.J., Jancar, S., 2013. Uptake of oxLDL and IL-10 Production by Macrophages Requires PAFR and CD36 Recruitment into the Same Lipid Rafts. Plos ONE 8, e76893.
Rothberg, K.G., Heuser, J.E., Donzell, W.C., Ying, Y.-S., Glenney, J.R., Anderson, R.G.W., 1992. Caveolin, a protein component of caveolae membrane coats. Cell 68, 673-682.
Saeki, K., Miura, Y., Aki, D., Kurosaki, T., Yoshimura, A., 2003. The B cell-specific major raft protein, Raftlin, is necessary for the integrity of lipid raft and BCR signal transduction. EMBO J. 22, 3015-3026.
Sargiacomo, M., 1993. Signal transducing molecules and GPI-linked proteins from a caveolin-rich insoluble complex in MDCK cells. J. Cell Biol. 122, 789-807.
Schuck, S., Honsho, M., Simons, K., 2006. Chapter 1 - Detergent-Resistant Membranes and the Use of Cholesterol Depletion, In: Celis, J.E. (Ed.), Cell Biology (Third Edition). Academic Press, Burlington, pp. 5-9.
Simons, K., Gerl, M.J., 2010. Revitalizing membrane rafts: New tools and insights. Nat. Rev. Mol. Cell Biol. 11, 688-699.
Simons, K., Ikonen, E., 1997. Functional rafts in cell membranes. Nature 387, 569-572.
Sonnino, S., Aureli, M., Grassi, S., Mauri, L., Prioni, S., Prinetti, A., 2014. Lipid Rafts in Neurodegeneration and Neuroprotection. Mol. Neurobiol. 50, 130-148.
Staubach, S., Hanisch, F.-G., 2011a. Lipid rafts: signaling and sorting platforms of cells and their roles in cancer. Exp. Rev. Proteom. 8, 263-277.
Staubach, S., Hanisch, F.G., 2011b. Lipid rafts: Signaling and sorting platforms of cells and their roles in cancer. Exp. Rev. Proteom. 8, 263-277.
Steigerova, J., Oklestkova, J., Levkova, M., Rarova, L., Kolar, Z., Strnad, M., 2010. Brassinosteroids cause cell cycle arrest and apoptosis of human breast cancer cells. Chem.-Biol. Interact. 188, 487-496.
Steinem, C., Janshoff, A., 2010. Multicomponent membranes on solid substrates: Interfaces for protein binding. Curr. Opin. Colloid Interface Sci. 15, 479-488.
Ulmer, C.Z., Jones, C.M., Yost, R.A., Garrett, T.J., Bowden, J.A., 2018. Optimization of Folch, Bligh-Dyer, and Matyash sample-to-extraction solvent ratios for human plasma-based lipidomics studies. Anal. Chim. Acta 1037, 351-357.
Vacek, J., Zatloukalová, M., Dorčák, V., Cifra, M., Futera, Z., Ostatná, V., 2023. Electrochemistry in sensing of molecular interactions of proteins and their behavior in an electric field. Microchim. Acta 190.
Vacek, J., Zatloukalova, M., Geleticova, J., Kubala, M., Modriansky, M., Fekete, L., Masek, J., Hubatka, F., Turanek, J., 2016. Electrochemical Platform for the Detection of Transmembrane Proteins Reconstituted into Liposomes. Anal. Chem. 88, 4548-4556.
Vacek, J., Zatloukalova, M., Kabelac, M., 2022. Redox biology and electrochemistry. Towards evaluation of bioactive electron donors and acceptors. Curr. Opin. Electrochem. 36.
Vainio, S., Bykov, I., Hermansson, M., Jokitalo, E., Somerharju, P., Ikonen, E., 2005. Defective insulin receptor activation and altered lipid rafts in Niemann–Pick type C disease hepatocytes. Biochem. J. 391, 465-472.

Varshney, P., Yadav, V., Saini, N., 2016. Lipid rafts in immune signalling: current progress and future perspective. Immunology 149, 13-24.
Watanabe, A., Tatematsu, M., Saeki, K., Shibata, S., Shime, H., Yoshimura, A., Obuse, C., Seya, T., Matsumoto, M., 2011. Raftlin is involved in the nucleocapture complex to induce poly(I:C)-mediated TLR3 activation. J. Biol. Chem. 286, 10702-10711.

Figures:

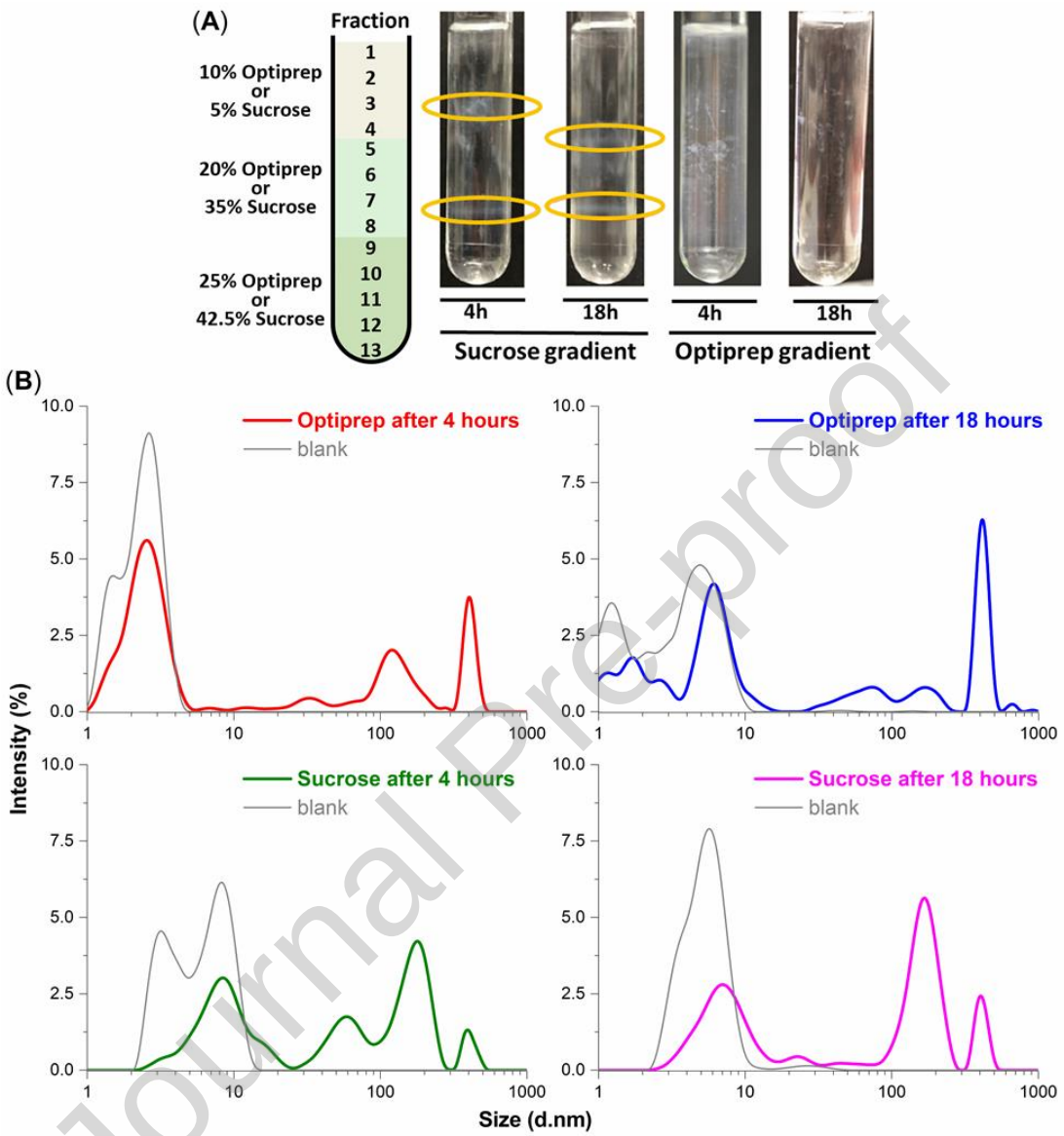

Fig. 1. (A) Schematic representation of distribution of individual fractions according to respective gradients (*left*) and real photos of tubes with orange highlighted areas rich in DRMs (*right*). **(B)** DLS particle size analysis in fraction 4. The presented DLS profiles were acquired as the average of four independent measurements at 20 °C.

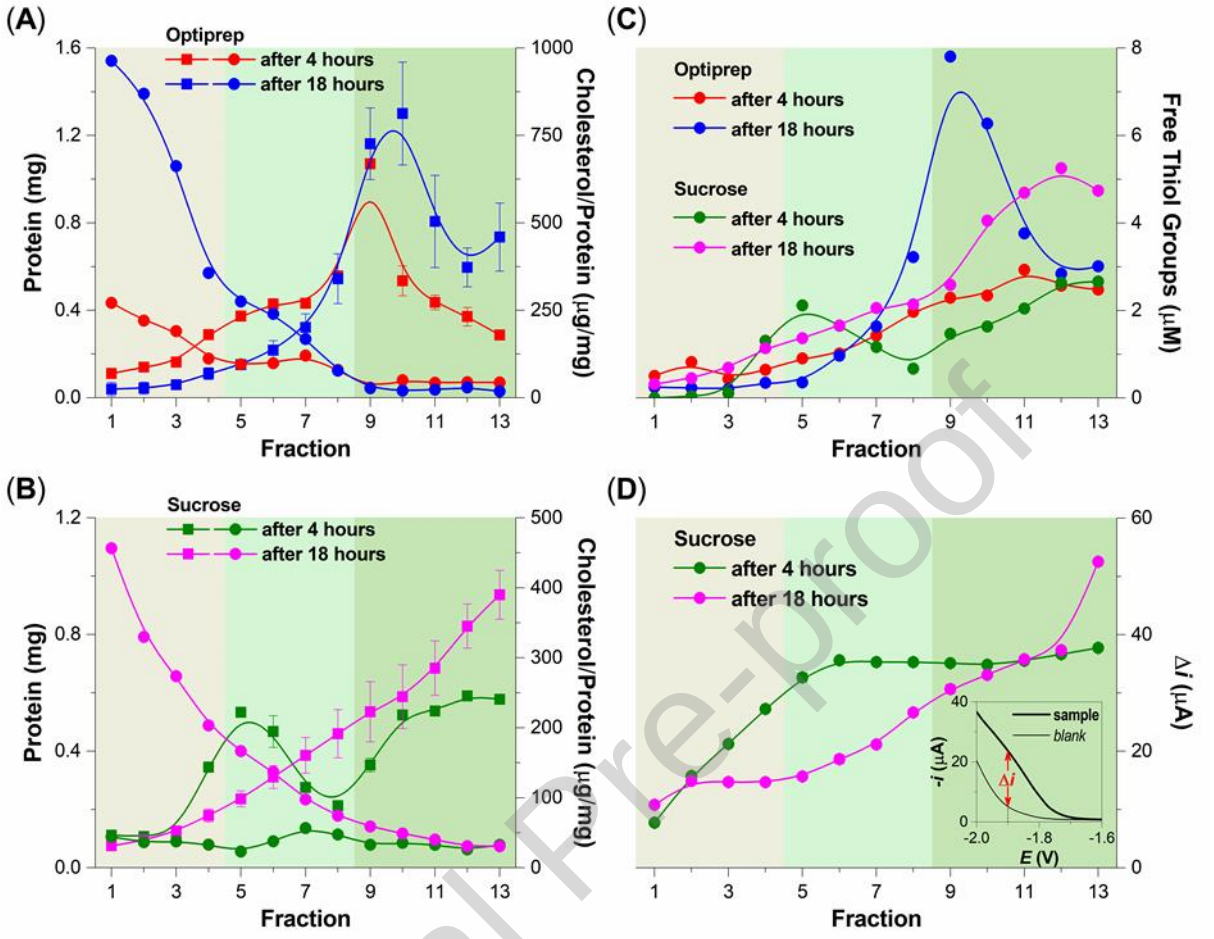

Fig. 2. Total protein amount (squares) and cholesterol content (in µg) per mg of protein (circles) in **(A)** Optiprep and **(B)** sucrose gradients after 4 or 18 hours of ultracentrifugation. Determination of **(C)** free thiols and **(D)** species involved in CHER using Ellman's reaction and voltammetric measurement, respectively. The inset in panel **D** shows how the Δ*i*-value was measured. For panels **A** and **B**, the data are expressed as the average (± SD) of three independent measurements for two and four independent DRMs isolations, respectively. In panels **C** and **D**, average values of three measurements for each fraction are presented. Error bars smaller than the plotted symbols are not visible.

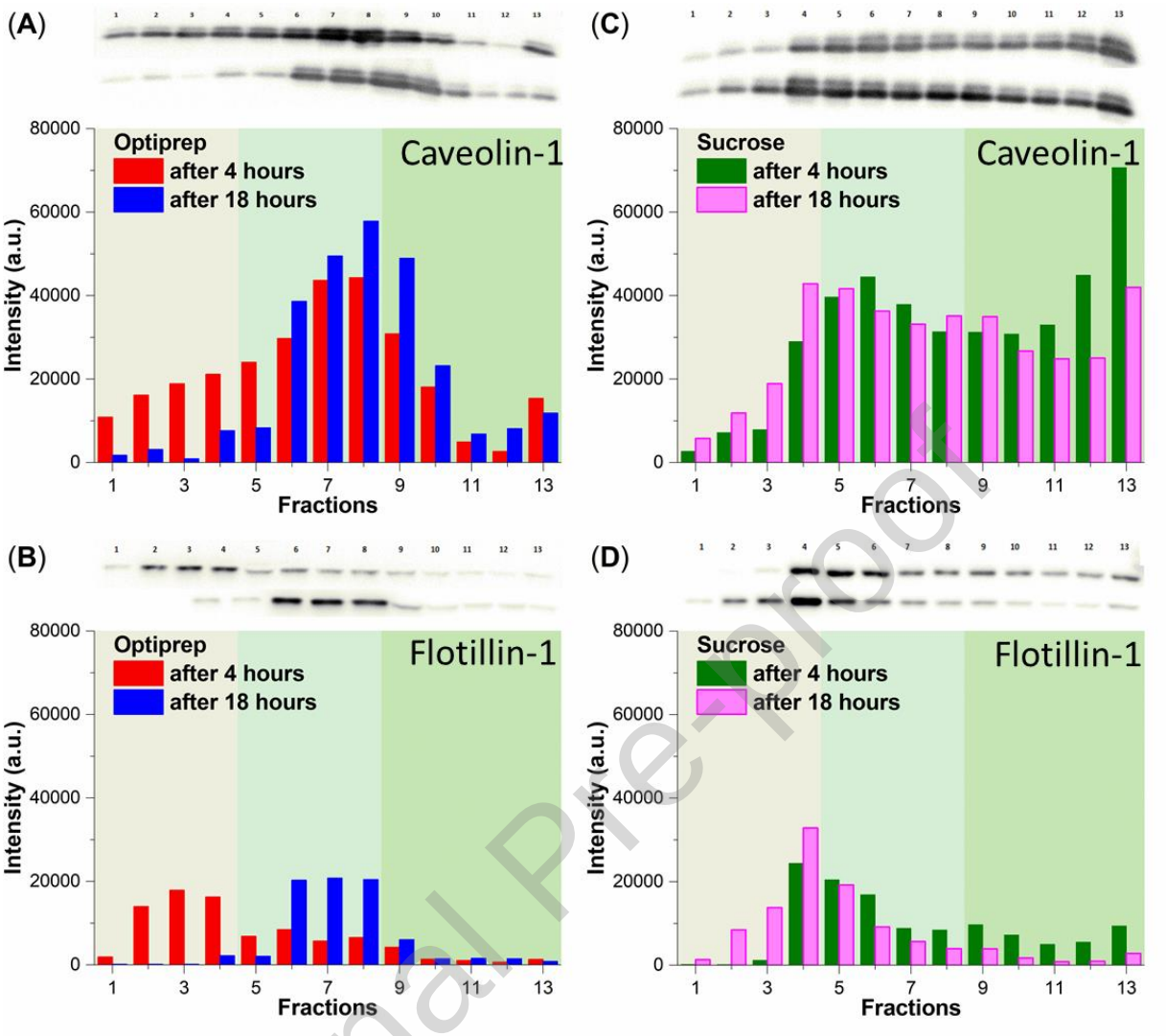

Fig. 3. Representative Western blot images (top: 4 h, down: 18 h) and quantification details of individual protein bands for **(A,C)** caveolin-1 and **(B,D)** flotillin-1 in **(A,B)** Optiprep and **(C,D)** sucrose gradients.

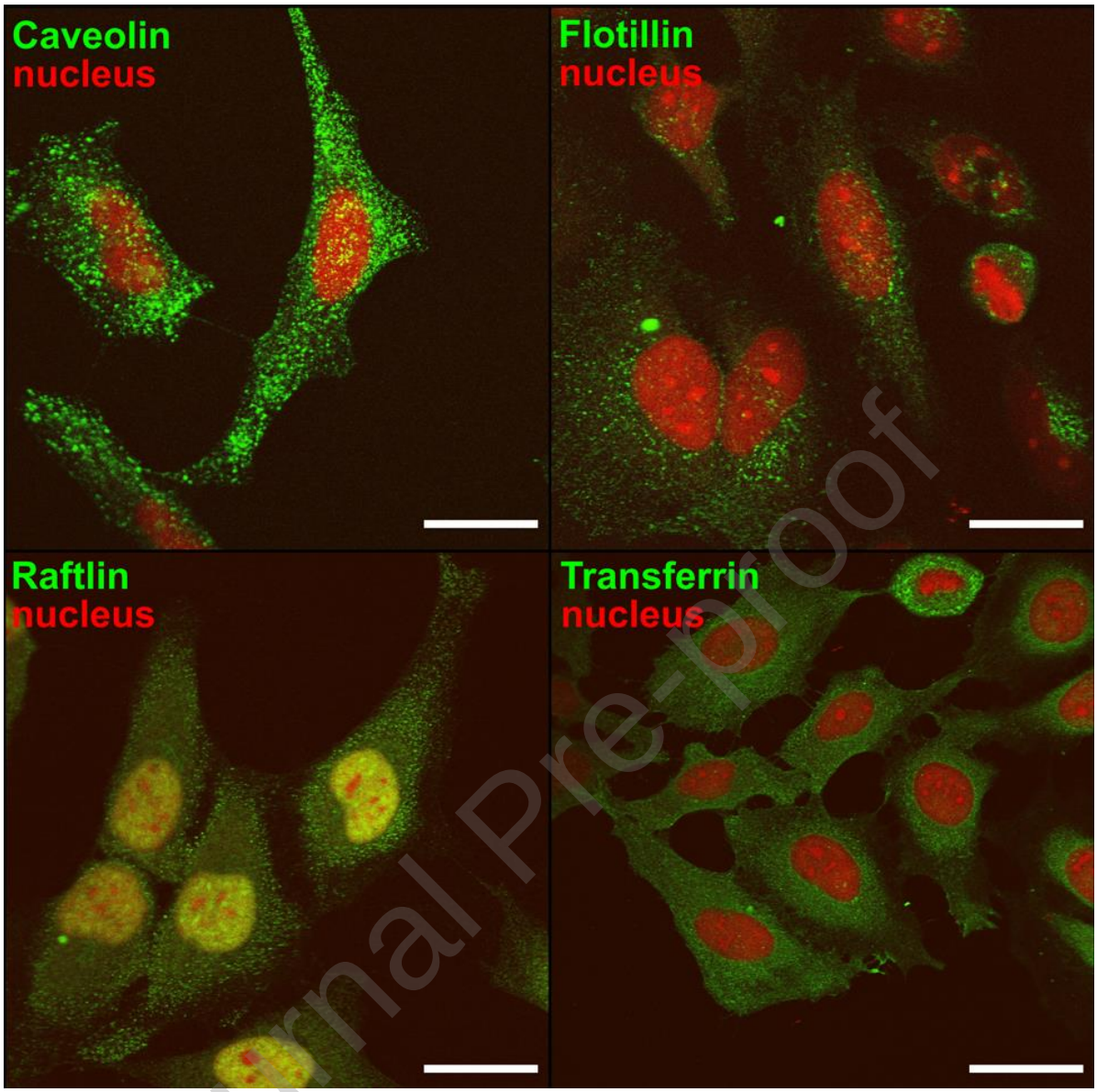

Fig. 4. Fluorescence microphotographs of caveolin-1, flotillin-1, raftlin, and transferrin localization (green) in Hela cells. Cells were visualized by laser-scanning confocal microscopy with cell nucleus staining with propidium iodide (red). Bar = 50 μm.

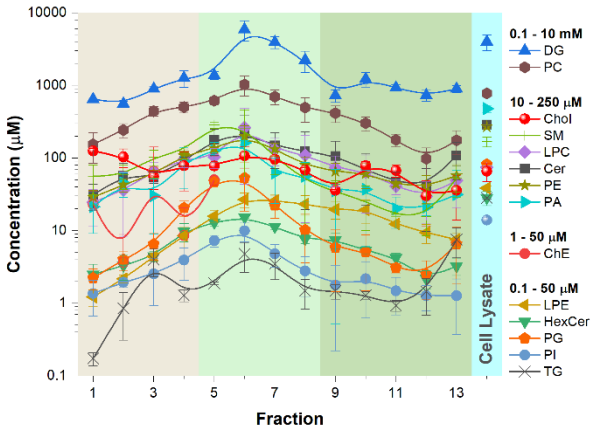

Fig. 5. Untargeted lipidomic LC-MS analysis. Estimated concentrations of putatively annotated lipid classes in individual fractions for sucrose gradient after 18 hours of ultracentrifugation. Ceramides (Cer), cholesterol (Chol), cholesterol ester (ChE), diacylglycerols (DG), hexosyl ceramides (HexCer), lysophosphocholines (LPC), lysophosphoethanolamines (LPE), phosphatidylglycerol (PG), phosphatidylinositol (PI), phosphocholines (PC), phosphoethanolamines (PE), phosphatidic acid (PA), sphingomyelins (SM), triacylglycerols (TG). Average values (± SD) of three independent experiments are presented. For total cholesterol content, see Figure 2B.

Declaration of Competing Interest

The authors declare that they have no known competing financial interests or personal relationships that could have appeared to influence the work reported in this paper.

Graphical abstract

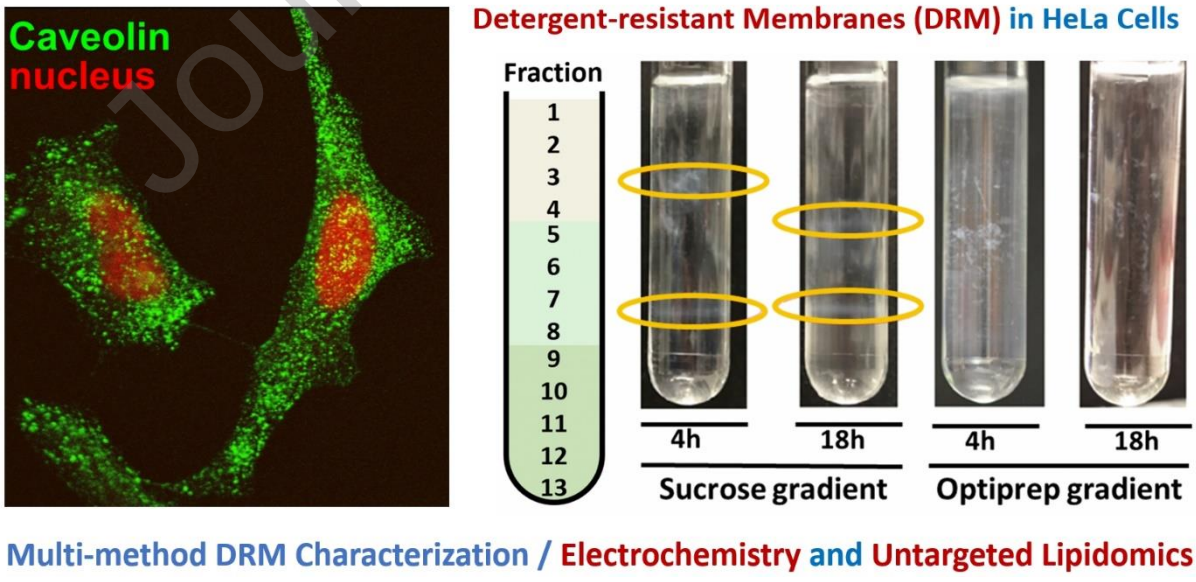

Highlights

- Two isolation protocols for detergent-resistant membranes (DRM) were compared.
- The study is based on a HeLa cell *in vitro* model.
- The results are supported by DRM protein marker subcellular imaging.
- Redox behaviour, electrocatalytic sensing and free thiol content is described for DRM.
- LC-MS-based untargeted lipidomic profiling of DRM is also demonstrated.